Many thanks to Referee #1 for appreciating our work and the very helpful comments that will significantly help to improve the manuscript!

Please find below our point-by-point reply to the reviewer concerns. Comments by Reviewer #1 are given in red, our reply is given in black, and changes in the manuscript are indicated in blue.

Reply to the Main Concerns by Reviewer # 1:

(General Comment 1:) Given the following points that are mentioned and discussed in the paper, I am wondering what value of a difference between zonal winds in Aeolus and reanalysis could be considered a (statistically) significant difference:
(a) The precision of Aeolus winds is about 3 to 7 m/s (line 104)
(b) The vertical and meridional components of winds are ignored (Eq. 3)
(c) The winds are interpolated to fixed geopotential heights (Eq. 4).

The following discussion has been included as a new Appendix B in the revised manuscript:

(a) Effect of precision:
Given a typical Aeolus along-track sampling of 90 km, about 5 Aeolus soundings per equator crossing fall into the 2S–2N latitude interval used for calculating the winds shown in Fig. 1 in the manuscript. According to the number of 15 orbits per day, there are 30 equator crossings per day. Further, our study is based on 7-day average winds. This means that a single Aeolus value shown in Fig. 1 is typically an average over 5x30x7 single soundings, i.e. about 1000 soundings. Assuming a precision of 7 $\mathrm{m\,s^{-1}}$, the precision of the 7-day zonal averages is 7 $\mathrm{m\,s^{-1}}$/ $\sqrt{1000}$, i.e. about 0.2 $\mathrm{m\,s^{-1}}$. This means that in Fig. 1 random errors are almost negligible.

(b1) Effect of vertical wind:
At altitudes 16–30 km the large scale upwelling in the tropics is weaker than about 0.1 $\mathrm{cm\,s^{-1}}$ (see Schoeberl et al., 2008). This contribution is much weaker than the zonal winds considered in our study and can therefore be neglected. In the troposphere, large-scale updrafts related to the Walker circulations are typically up to about 0.01 $\mathrm{m\,s^{-1}}$ (e.g., Wang, 2002; Eresanya and Guan, 2021), i.e., also relatively weak. Locally, stronger updrafts and downdrafts can occur particularly in the troposphere during deep convective events, or generally in atmospheric gravity waves. The effect of such events should occur as quasi-random fluctuations in the Aeolus HLOS winds and should therefore cancel out in averages. In the zonal wavenumber–frequency spectra, they should contribute to the uniform spectral background that can be seen, for example, in former Fig. 6.
It should however be kept in mind that small-scale fluctuations due to vertical winds should already be strongly suppressed because the Aeolus Rayleigh winds provided as Level 2B data are averages over 86.4 km intervals along-track (Lux et al., 2020). Therefore the effect of local thunderstorms should average out. In addition, vertical motions associated with strongly convective cloud systems and large-scale fronts often occur below cloud tops, where Aeolus does not provide observations of Rayleigh winds (see also Rennie et al., 2022).

(b2) Effect of meridional wind:
As already stated in Sect. 2.1 in the manuscript, in the tropics Aeolus is about 6 times more sensitive to zonal winds than to meridional winds. Therefore biases due to meridional winds should generally be small. In particular, in zonal averages, like those shown in Fig. 1 in the manuscript, the meridional wind components of atmospheric waves should cancel out.
In the new Appendix B we have included time series of 7-day average meridional winds observed at the 8 radiosonde stations considered in our study. In the stratosphere, these meridional winds are usually weaker than about 3 $\mathrm{m\,s^{-1}}$. Given the 6 times stronger sensitivity of

Aeolus to tropical zonal wind than to tropical meridional wind, biases due to meridional winds should be weaker than about 0.5 m s^{-1}. In the troposphere, the 7-day average meridional winds can be stronger (as strong as about 6 to 10 m s^{-1}). Therefore locally biases of the zonal wind of up to 1 to 1.5 m s^{-1} can be expected. On zonal average, however, there should be strong cancellation effects, resulting in much weaker biases.

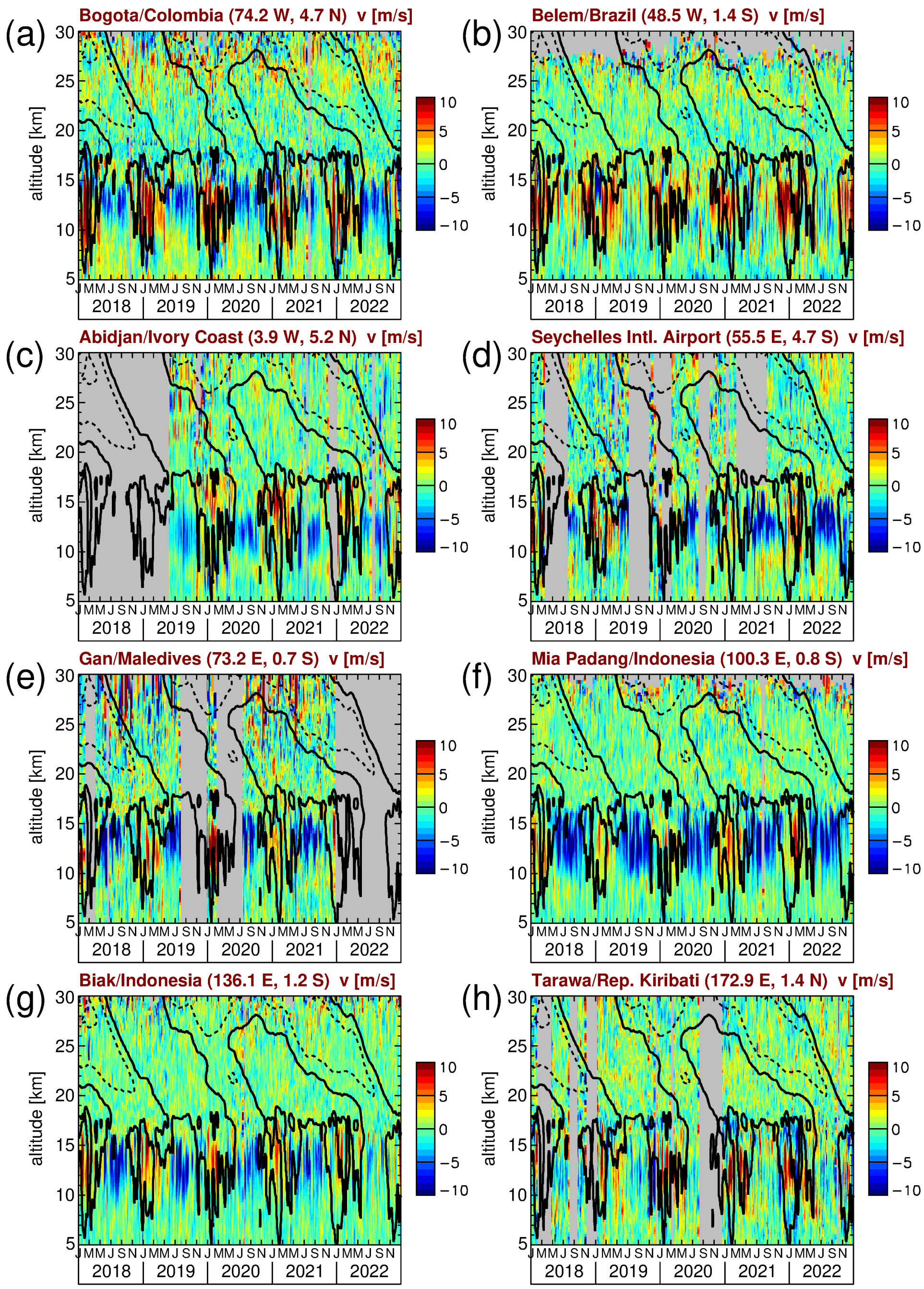

Figure 1: Meridional wind observed at the eight radiosonde stations introduced in Fig. 2 in the manuscript. Contour lines indicate the ERA-5 zonal mean zonal wind shown in Fig. 1a in the manuscript.

(c) Interpolation to fixed geopotential heights:

Of course, there will be differences in the temperature-pressure profiles between the different reanalyses, resulting in slight shifts of the altitude coordinates.

As a measure of uncertainty, for the reanalyses we have calculated at given geopotential altitudes the pressure differences between reanalysis and different radiosonde stations as a reference. These pressure differences were then converted into altitude differences using the local scale height. This has been performed for the dataset of 7-day averages calculated with a time step of three days. The characteristics found for the different radiosonde stations are very similar. Therefore we only show the differences for the Tarawa station because the zonal wind differences at Tarawa are relatively strong (see former Fig. 5e–h).

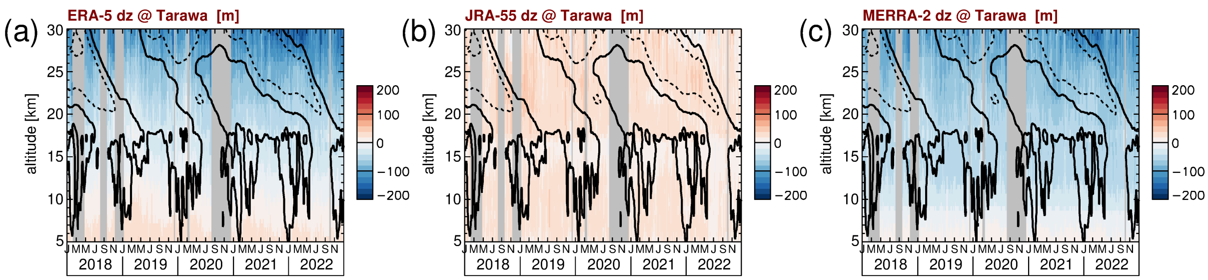

Figure 2: Differences in geopotential altitude between **(a)** ERA-5, **(b)** JRA-55, and **(c)** MERRA-2 and the radiosondes at Tarawa as a reference. Altitude differences were calculated from pressure differences at given geopotential altitudes using the local scale height. Zonal wind contour lines are from ERA-5. Contour interval is 20 m s^{-1}, westward winds are indicated by dashed contour lines, and zero wind is indicated by solid contour lines.

As can be seen from this figure, the altitude differences show a systematic pattern with only small temporal variations. Deviations are typically less than 100 m with JRA-55 showing the smallest deviations on average (possibly because JRA-55 assimilates IGRA radiosonde data). Given typical magnitudes of QBO-related vertical gradients of the zonal wind of about 10 m s^{-1} km^{-1} (perhaps 20 m s^{-1} km^{-1} at maximum), this would result in typical biases of 1 to 2 m s^{-1}, which is much less than the biases seen for JRA-55. This is some evidence for systematic errors in the zonal momentum budget of JRA-55 being the dominant effect responsible for the wind biases seen in the QBO shear zones. Also for the other reanalyses errors in the zonal momentum budget will contribute to the wind differences seen in the zones of strong wind shear.

It should also be mentioned that Aeolus observations are given on geometric altitudes (see also Rennie et al., 2020). At $\sim$20 km altitude geometric altitudes deviate by about 100 m from geopotential altitudes. This deviation is of similar magnitude as the differences in geopotential altitude between radiosondes and reanalyses. Therefore, in the QBO shear zones also differences of about 1 to 2 m s^{-1} can be expected when comparing Aeolus with datasets given on geopotential height.

(General Comment 2) Has any kind of tapering been applied to the 31-day period windows before applying the 2D Fourier transforms? If not, do you see any spectral leakage at higher frequencies?

In order to preserve the variances of the data contained in the 31-day period windows no tapering has been applied. We did not notice any effects of spectral leakage at higher frequencies. It can also be seen from the spectra in former Fig. 6 that there are no indications for spectral leakage. In addition, it should be kept in mind that in this study we are only interested in relatively low frequencies: $<$0.15 cycles day^{-1} for equatorial Rossby waves, and $<$0.3 cycles day^{-1} for Kelvin waves. Only for MRGWs and n=0 IGWs frequencies as high as 0.45 and 0.5 cycles day^{-1}, respectively, are used.
This information has been added in the revised manuscript at the end of Sect. 4.1.

(General Comment 3) Related to the point above, when a 31-day window is being used, and assuming no tapering in time, the lowest resolved frequency should be 0.03 cycles/day. However, in isolating the Kelvin waves, the frequency of 0.015 cycles/day has been used as the lower band (i.e., a period of 67 days). I think this results in some contamination of the Kelvin wave signal by the quasi-stationary waves.

We calculate Fourier frequencies in steps of 31^{-1} cycles day^{-1}, which is the frequency resolution given by the length of the 31-day time windows. The number of 0.015 cycles day^{-1} is just given for technical reasons and corresponds to half of the frequency resolution of our spectra. In order to perform an integration in the spectral domain, an area has to be assigned to the discrete Fourier frequencies, which is given by the spectral resolution in zonal wavenumber and frequency, i.e. “1” for zonal wavenumber and 31^{-1} cycles day^{-1} for frequency. In particular, this means that for the traveling waves the spectral contributions at zero frequency, i.e., the stationary waves, are not used even though we state for the Kelvin and equatorial Rossby wave modes half the frequency resolution as the lower integration boundary.

This information has been added in the revised manuscript in Sect. 4.2.2. Further, we now state the more correct value of 62^{-1} cycles day^{-1} that was actually used (half the frequency resolution) as the lower frequency boundary for the integration domains of the Kelvin and equatorial Rossby waves.

Reply to the Specific Comments by Reviewer # 1:

(1) Line 52: It might be useful to mention that the gravity waves are usually not resolved in climate models and their effects are approximated using different parameterization schemes.

As recommended by the reviewer, this is now stated in the revised manuscript.

(2) Lines 130 to 150: My understating is that the Aeolus and radiosondes winds are interpolated to 0.25 km vertical resolution, but the reanalysis are interpolated to a 0.5 vertical resolution. If this is the case, then how you subtract them in the next sessions?

The differences are calculated only for the altitude levels that are common to both data sets.

This is now stated in the revised manuscript in the first paragraph of Sect. 2.3.

(3) Figure 1: I am not sure why the one standard deviation is shown with respect to zero. I think it should be shown with respect to the mean differences (i.e., the red line).

The intention of Fig. 1 in the manuscript is to show both the systematic deviations (on long-term average) and the standard deviation with Aeolus as a reference. For this purpose, the standard deviation is calculated with respect to the zero line, i.e. Aeolus as a reference. It was not our intention to show how robust (in a statistical sense) the systematic differences between Aeolus and the reanalyses are.

This is now stated more clearly in the revised manuscript.

(4) Figure 6: Have you tried using a log-scale for plotting the power? I think it would be useful in extracting the interesting features in higher frequencies.

Linear scales were used intentionally to show the features of the MRGWs and n=0 IGWs at higher frequencies. As can be seen from former Fig. 6, the problem is that in the antisymmetric spectrum there is a relatively high uniform spectral background of about 3.5 $m^2\,s^{-2}$/wavenumber/(cycles/day). The peak spectral densities of MRGWs and IGWs are at about 5 and 4.5, respectively, in the same units, i.e., not much higher. Using a logarithmic scale would therefore obscure the MRGW and IGW signals.

No changes were made in the revised manuscript.

(5) Section 4.2.4. You might want to mention that the peak variances at 30 km are due to extratropical Rossby waves propagating equatorward from the winter hemisphere and are not related to the equatorial Rossby waves.

This is now mentioned in the revised manuscript.

(6) Figure A2: I am a little bit surprised by the panel for MRGW. I expected to see a stronger signal in meridional wind than in the zonal wind for MRG waves. In isolating the MRG signal based on the wavenumber-frequency spectrum, have you considered the fact the MRG waves are symmetric in meridional wind (while they are antisymmetric in zonal wind)?

We are sorry for not stating explicitly enough the intention of Appendix A2!
Figure A2 was meant to show that meridional wind components in the same spectral band and of the same symmetry as the zonal wind variances shown in Sect. 4.2 will not significantly contaminate the zonal wind variances shown in Sect. 4.2. This means that, for this purpose,

we have to integrate over the same spectral bands as for the zonal wind variances, and **we also have to use the same symmetry as for the zonal winds**. This is why we have to investigate the antisymmetric contribution of the meridional wind variances in the MRGW spectral wave band. Of course, this contribution is relatively small because MRGWs are symmetric in meridional winds. The same holds for the n=0 IGWs. Further, it should be mentioned that the meridional wind variances in Fig. A2b are so strong because the symmetric meridional wind signal of the equatorial Rossby wave mode that is antisymmetric in zonal wind, but symmetric in meridional wind is picked up. Still, this meridional wind signal would not significantly affect the zonal wind variances of the symmetric (in zonal wind) equatorial Rossby waves. Similarly, the meridional wind variances in Fig A2e (MRGWs) are likely due to the antisymmetric meridional wind signal of the equatorial Rossby wave mode that is symmetric in zonal wind.

Indeed, for MRGWs symmetric meridional wind variances are somewhat stronger than the antisymmetric zonal wind variances. For example, Kim et al. (2019) find meridional wind variances between 2 and 3 $m^2\,s^{-2}$ on 15S–15N average for different reanalyses in the tropopause region at 100 hPa. These numbers are similar to the zonal wind peak variances found in our study. Further, also Kim et al. (2019) find that, compared to other reanalyses, JRA-55 has relatively weak MRGW variances.

This more detailed discussion has been included in the revised Appendix A2.

(7) Line 207: The comma before "Also", should change to a dot.

done

References

Eresanya, E. O. and Guan, Y.: Structure of the Pacific Walker Circulation depicted by the reanalysis and CMIP6, Atmosphere, 12, 1219, https://doi.org/10.3390/atmos12091219, 2021.

Kim, Y.-H., Kiladis, G. N., Albers, J. R., Dias, J., Fujiwara, M., Anstey, J. A., Song, I.-S., Wright, C. J., Kawatani, Y., Lott, F., and Yoo, C.: Comparison of equatorial wave activity in the tropical tropopause layer and stratosphere represented in reanalyses, Atmos. Chem. Phys., 19, 10027–10050, https://doi.org/10.5194/acp-19-10027-2019, 2019.

Lux, O., Lemmerz, C., Weiler, F., Marksteiner, U., Witschas, B., Rahm, S., Geiß, A., and Reitebuch, O.: Intercomparison of wind observations from the European Space Agency's Aeolus satellite mission and the ALADIN Airborne Demonstrator, Atmos. Meas. Tech., 13, 2075–2097, https://doi.org/10.5194/amt-13-2075-2020, 2020.

Rennie, M., Tan, D., Andersson, E., Poli, P., Dabas, A., de Kloe, J., Marseille, G.–J., and Stoffelen, A.: Aeolus Level-2B algorithm theoretical basis document (Mathematical description of the Aeolus L2B processor), ECMWF report, AED-SD-ECMWF-L2B-038, Version: 3.40, available at: https://earth.esa.int/eogateway/documents/20142/37627/Aeolus-L2B-Algorithm-ATBD.pdf (last access: 06 June 2023), 2020.

Rennie, M., Healy, S., Abdalla, S., McLean, W., and Henry, K.: Aeolus positive impact on forecasts with the second reprocessed dataset, ECMWF newsletter, No. 173, 14–20, doi:10.21957/mr5bjs29fa, 2022.

Schoeberl, M. R., Douglass, A. R., Stolarski, R. S., Pawson, S., Strahan, S. E., and Read, W.: Comparison of lower stratospheric tropical mean vertical velocities, J. Geophys. Res., 113, D24109, doi:10.1029/2008JD010221, 2008.

Wang, C.: Atmospheric circulation cells associated with the El Nino–Southern Oscillation, J. Climate, 15, 399–419, 2002.